Corrigendum to "Consumption in Asset Returns"

SVETLANA BRYZGALOVA, JIANTAO HUANG, and CHRISTIAN JULLIARD*

ABSTRACT

This corrigendum documents two numerical issues in the replication package for Bryzgalova, Huang, and Julliard (2026, BHJ). We correct a double-log transformation in the baseline stock-and-bond cross-section and an argument-passing issue in the Epstein-Zin risk-free-rate calibration under stochastic volatility. We rerun the affected replication codes and find that the main empirical estimates and economic conclusions are essentially unchanged. The risk-free-rate calibration in the stochastic-volatility panels becomes slightly closer to the historical average.

*Svetlana Bryzgalova is with the Department of Finance, London Business School, and CEPR. Jiantao Huang is with the Faculty of Business and Economics, the University of Hong Kong. Christian Julliard is with the Department of Finance, London School of Economics.

Summary

1. **Double-log correction.** We correct a data-transformation issue in the original BHJ replication package. In several scripts for the baseline cross-section of 37 stock plus nine bond portfolios, the code applies $\log(1+x)$ even though x is already a log excess return. This produces a "double-log" transformation of the baseline stock-and-bond returns. In our replication, we replace these lines by the corresponding log-return series directly. This correction affects the baseline 46-asset stock-and-bond cross-section, but it does not affect the Kozak et al. (2020) 74 anomaly portfolio analysis, where the relevant return transformations are handled separately. After making this correction, we reran the affected replication codes underlying Figure 2, Figures 5–16, and Tables III–VII. The resulting impulse responses, moving-average consumption component, return loadings, variance decompositions, stochastic-volatility estimates, and structural calibration results are quantitatively nearly indistinguishable from those reported in the published paper. Thus, while the original transformation generates an approximation error, correcting it does not alter the empirical conclusions.

2. Moreover, this data-transformation issue does not appear in the analysis of shareholders' and nonshareholders' consumption growth (Figure 4 and Table VII, Panel E), nor in the mixed-frequency state-space exercises reported in Figure 6 and Figure 7. It also does not affect the main cross-sectional risk-price estimates in Table V.[1]

3. **Risk-free-rate calibration in Table 7 Panels B and D.** We correct a minor input error in the Epstein–Zin risk-free-rate calculation for the stochastic-volatility panels. In the original code, Panels B and D use consumption-growth variance in place of wealth-return variance. We correct this typo so that the risk-free-rate calculation follows the formula stated in the paper. This lowers the annualized risk-free-rate calibration in Panels B and D from about 2.08–2.16% to 1.67–1.79%, closer to the historical average of 1.68%. The substantive conclusions are unchanged.

[1] Separately, we note that the original Table V code applies the Jensen adjustment for long-short composite portfolios using $\frac{1}{2}\operatorname{Var}(r_L - r_S)$, whereas a leg-by-leg approximation implies the convexity term $\frac{1}{2}\left[\operatorname{Var}(r_L) - \operatorname{Var}(r_S)\right]$. This adjustment affects only the long-short composite panels, Panels C and E. The Panel E median risk-price estimate changes from 0.276 to 0.253, while the Panel C median is almost unchanged. We do not report these results separately, because we view this as an alternative Jensen-approximation convention rather than a coding correction. The qualitative conclusions are unaffected.

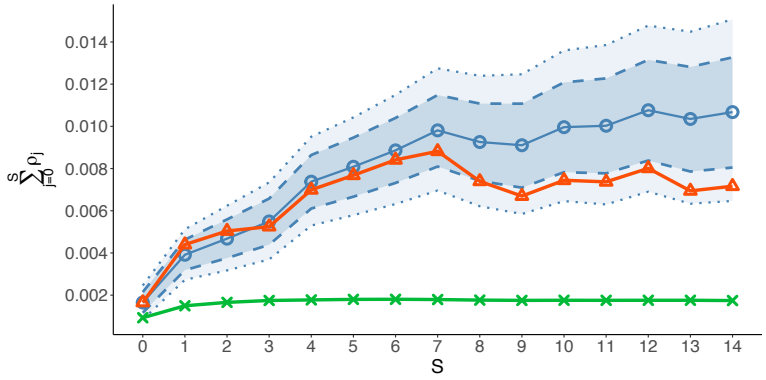


Figure 2. Cumulative impulse response function of consumption growth to a one-standard-deviation shock spanned by asset returns. This figure plots the posterior means of the cumulative response function of consumption growth (solid line with circles), with the centered posterior 90% (dotted lines) and 68% (dashed lines) coverage regions. The red line with triangles denotes the first principal component of $cov(r^{ex}_{i,t}, \Delta c_{t,t+1+S})$. The data are quarterly data (1963:Q3 to 2019:Q4). The green line with crosses is the simulated cumulative impulse responses assuming that (i) monthly consumption growth is independent over time and has a contemporaneous correlation of 0.20 with the monthly f_t shock, and (ii) monthly consumption data are benchmarked to the annual data (see Internet Appendix Section VIII for details).

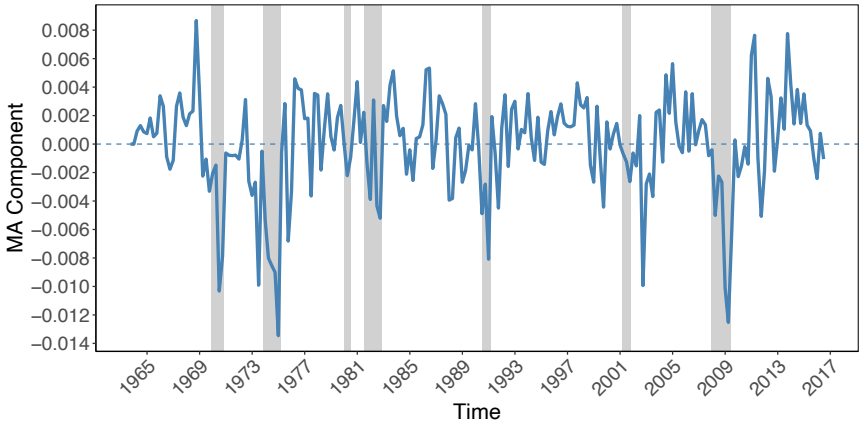


Figure 5. Moving average component of consumption growth. This figure plots the posterior mean of the moving average f_t component of consumption growth. Grey areas denote NBER recessions. Estimates are based on the single-factor model in equations (2) and (3), with $\bar{S} = 14$. The cross-section of base assets includes 25 size- and value-sorted portfolios, 12 industry portfolios, and nine bond portfolios.

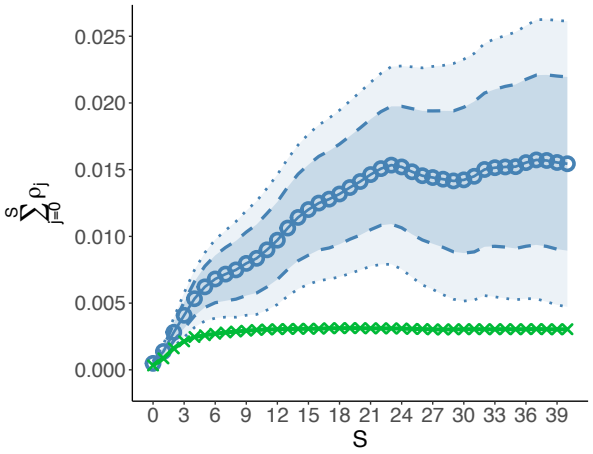


Figure 6, Panel B. Implied CIRFs based on monthly estimates in Figure IA.3 This figure plots the posterior means of the cumulative IRF of quarterly consumption growth (solid lines with circles) to monthly asset return shocks, with centered posterior 90% (dotted lines) and 68% (dashed lines) coverage regions. The x-axis denotes the number of *monthly* lags. Panel B is based on the impulse responses of monthly consumption growth to monthly asset return shocks, converted into the CIRFs of quarterly consumption growth to monthly asset return shocks (see equation (IA.15) of the Internet Appendix). Green lines display the simulated cumulative impulse responses, assuming that (i) monthly consumption growth is independent over time and has a contemporaneous correlation of 0.20 with the monthly f_t shock, and (ii) monthly consumption data are benchmarked to the annual data (see Internet Appendix VIII for details).

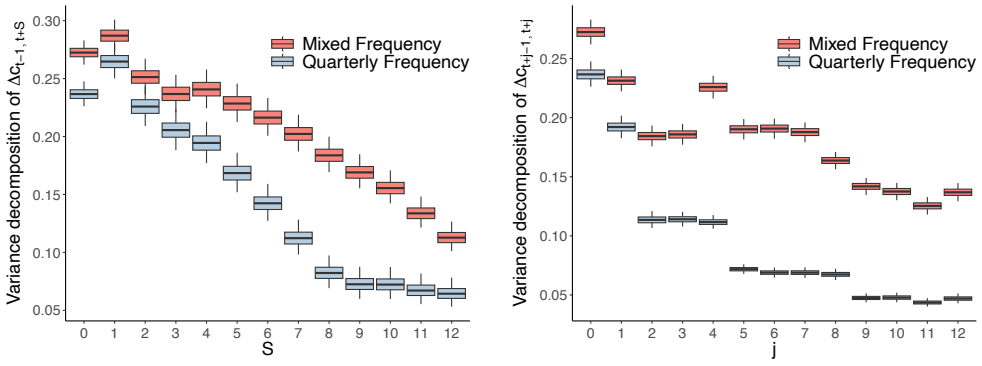


Figure 7. Share of consumption growth variance driven by its moving average component. This figure presents box plots (posterior 95% coverage area) of the percentage of time-series variances of consumption growth explained by the MA component. The state-space models are estimated at both quarterly (blue bars) and mixed (red bars) frequencies. The plots report the unadjusted R^2. Left panel: Cumulated consumption growth $\Delta c_{t-1,t+S}$. Right panel: One-period consumption growth $\Delta c_{t-1+j,t+j}$. Estimates are based on a single-factor model, with $\bar{S} = 14$. The cross-section of base assets includes 25 size- and value-sorted portfolios, 12 industry portfolios, and nine bond portfolios.

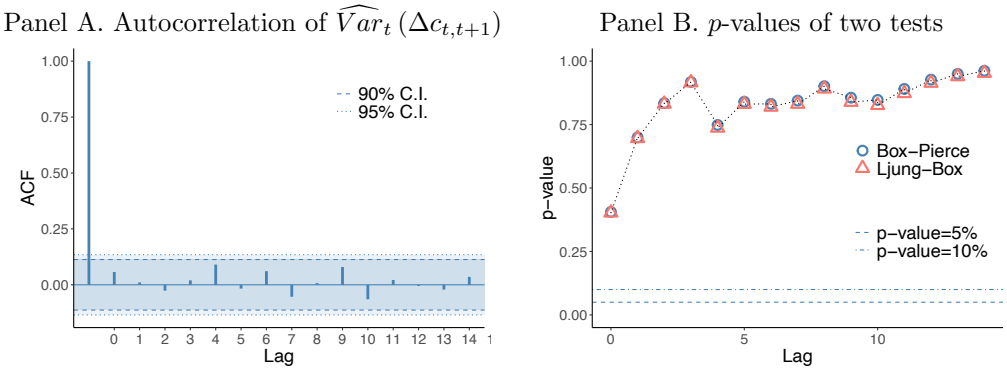


Figure 8. Autocorrelation structure of consumption growth squared forecast errors. Panel A: Autocorrelation function of $\widehat{Var}_t(\Delta c_{t,t+1})$ with 95% and 99% confidence bands. Panel B: p-values of Ljung and Box (1978) (red triangles) and Box and Pierce (1970) (blue circles) tests.

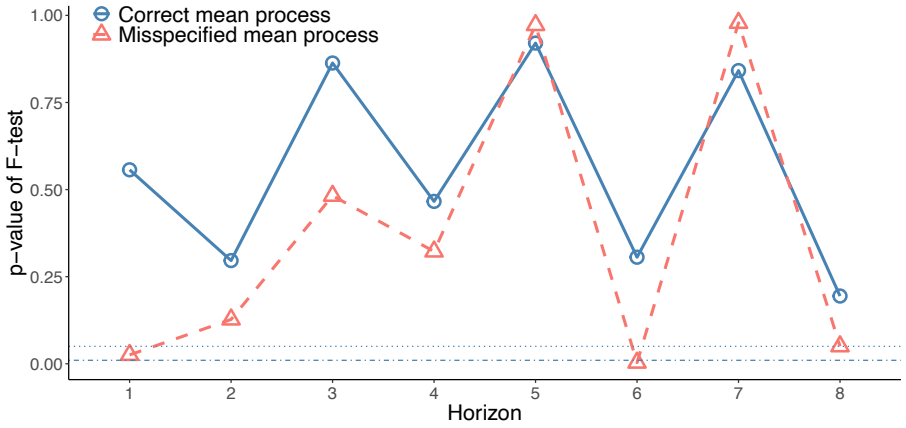


Figure 9. Predictability of consumption squared forecast errors. This figure plots predictive regressions of $\widehat{Var}_{t+h}(\Delta c_{t+h,t+h+1})$ on the time-t first eight PCs of asset returns at several horizons h. We report the p-value of the F-test of the joint significance of the covariates as well as the 5% and 1% significance thresholds (respectively, horizontal dot-dashed and dotted lines). The solid blue line with circles denotes statistics for the correctly specified conditional mean for the consumption growth process. The dashed red line with triangles corresponds to the assumption of a constant conditional mean.

Table III, Panels B and C. Estimates of ARCH(1), GARCH (1,1), and IGARCH(1,1) for Different Models

This table reports ARCH(1), GARCH(1,1), and IGARCH(1,1) estimates for consumption growth volatility with different models for the conditional mean. Models are estimated via quasi-maximum likelihood estimator (QMLE). Robust standard errors are constructed using Newey and West (1987). The table also reports Akaike, Bayesian, Shibata, and Hannan-Quinn information criteria.

$$\Delta c_{t+1} = \mu_t + \epsilon_{t+1}$$
$$\sigma^2_{t+1} = \omega + \alpha\epsilon^2_t + \beta\sigma^2_t$$

	ARCH(1)		GARCH(1,1)			IGARCH(1,1)		
	ω	α	ω	α	β	ω	α	β
	(1)	(2)	(3)	(4)	(5)	(6)	(7)	(8)
Panel B: $\mu_t = \mu_0 + \mu^c_1 \Delta c_t + \sum_{i=1}^{8} \mu^r_i r^{ex}_{PC_i,t}$								
Estimate	0.905	0.084	0.000	0.000	0.999	0.000	0.000	1.000
Std error	(0.138)	(0.084)	(0.001)	(0.000)	(0.000)	(0.000)	(0.004)	(0.004)
Akaike		2.842			2.852			2.852
Bayes		2.874			2.900			2.884
Shibata		2.842			2.852			2.852
Hannan-Quinn		2.855			2.871			2.865
Panel C: $\mu_t = \mu_0 + \sum_{i=1}^{S} \rho_i f_{t+1-i}$								
Estimate	0.883	0.124	0.000	0.000	0.999	0.000	0.019	0.981
Std error	(0.145)	(0.104)	(0.001)	(0.000)	(0.000)	(0.000)	(0.067)	(0.067)
Akaike		2.842			2.850			2.855
Bayes		2.874			2.897			2.887
Shibata		2.842			2.849			2.855
Hannan-Quinn		2.855			2.869			2.868

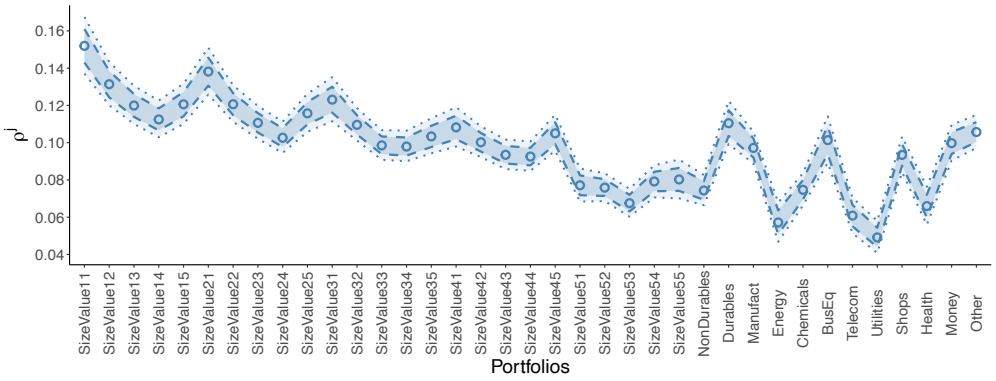


Figure 10. Common factor loadings (ρ^r) of the stock portfolios in the one-factor model. This figure plots the posterior means of the stock factor loadings on f_t (circles) and centered posterior 90% (dashed line) and 68% (dotted line) coverage regions in the one-latent-factor model. Ordering of portfolios: 25 Fama and French (1992) size- and book-to-market-sorted portfolios and 12 industry portfolios.

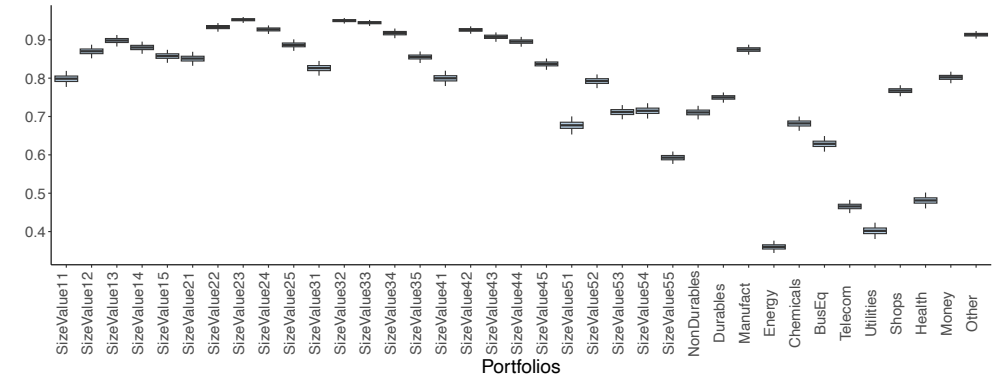


Figure 11. Share of stock portfolios' return variance explained by the f component. This figure plots box-plots (posterior 95% coverage area) of the percentage of time-series variances of individual stock portfolio returns explained by the f component in the one-factor model. Ordering of portfolios: 25 Fama and French (1992) size- and book-to-market-sorted portfolios and 12 industry portfolios.

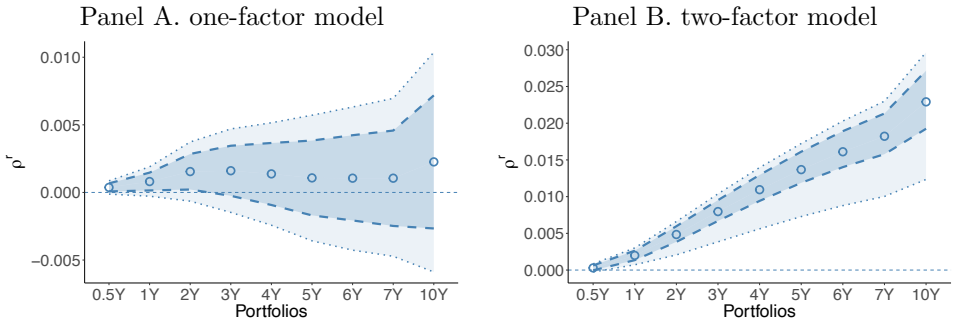


Figure 12. Bond loadings on common factor f_t. The figure shows posterior means of the bond factor loadings on f_t (blue circles) and centered posterior 90% (dashed line) and 68% (dotted line) coverage regions in the one- and two-factor models.

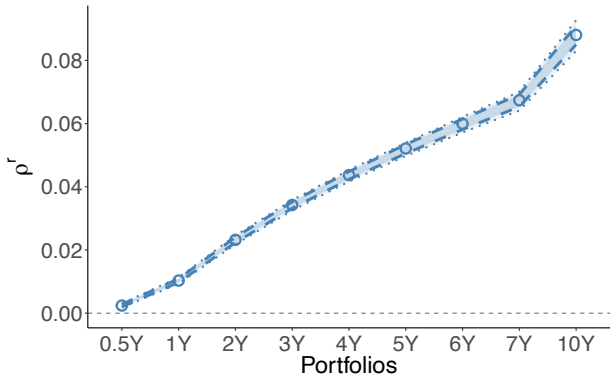


Figure 13. Bond loadings ($\boldsymbol{\theta}^b$) on the bond-specific factor (b_t). The figure shows posterior means (blue circles), and the centered posterior 90% (dashed line) and 68% (dotted line) coverage regions, of bond loadings on the bond-specific factor b_t.

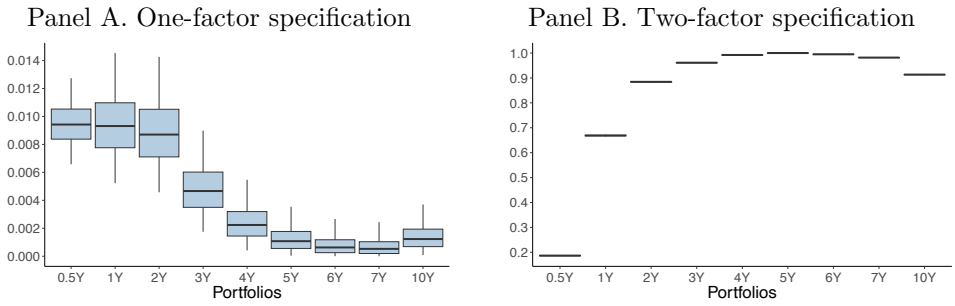
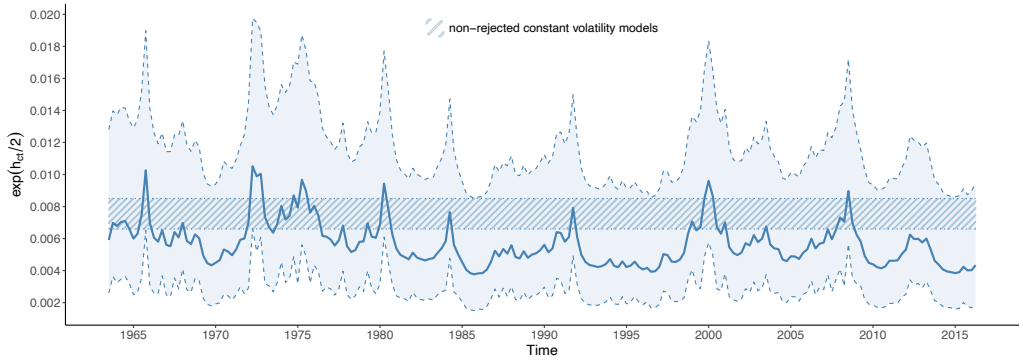
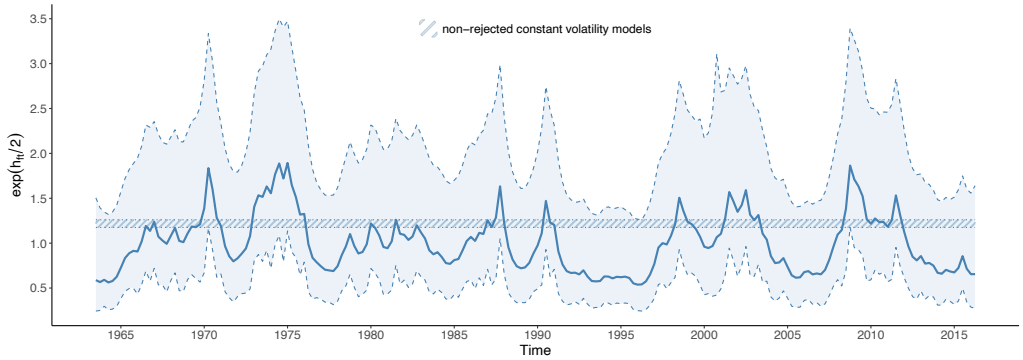


Figure 14. Variance decomposition box plots of bond returns. The figure shows box plots (posterior 95% coverage area) of the percentage of time-series variances of bond returns explained by the f_t (Panel A) and f_t and b_t (Panel B) shocks.

Panel A: Log volatility of the short-run consumption shock (w_t^c) in equation (2)



Panel B: Log volatility of the shock to the conditional mean of consumption growth (f_t)



Panel C: Common log volatility of asset return (h_{rt} in equation (19))

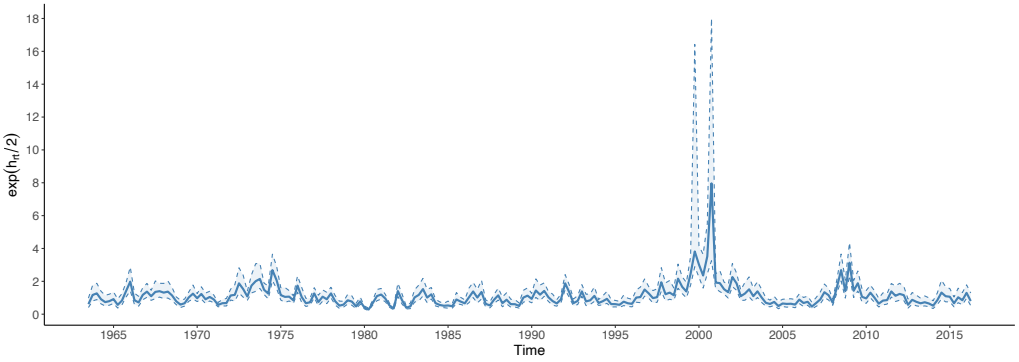
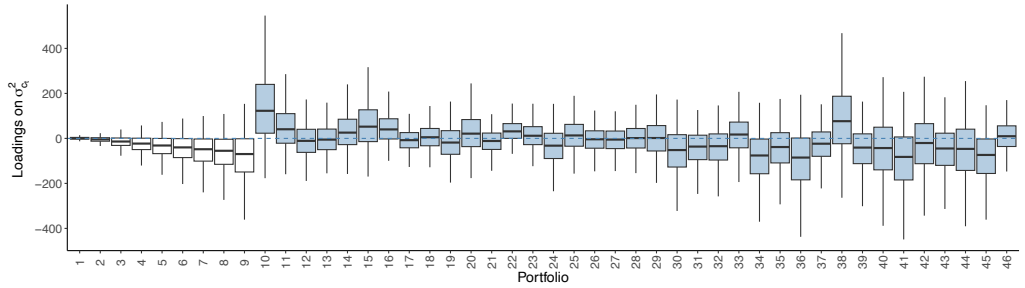
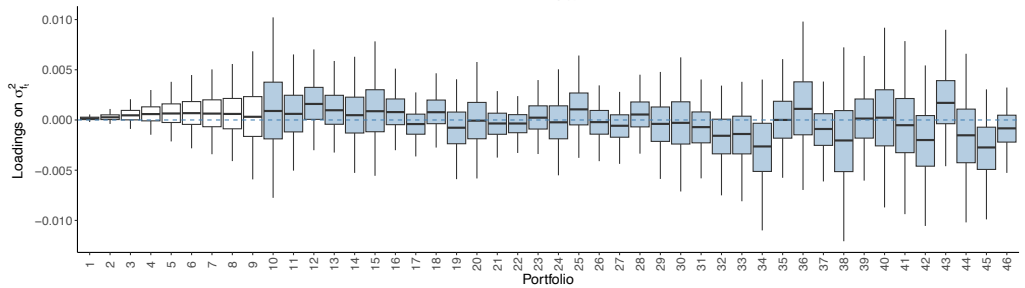


Figure 15. Filtered stochastic volatilities of consumption and returns. The figure shows the estimated stochastic volatilities of the model in equations (2) and (16) to (19), and Section II.B of the Internet Appendix under a diffuse prior for the autoregressive volatility coefficients. Solid blue lines depict the posterior median of the log volatility, whereas dotted red lines denote 2.5% and 97.5% credible intervals. Shaded (patterned) areas reflect constant volatility levels that would not be rejected given the credible intervals.

Panel A: Posterior distribution of excess return loadings ($\boldsymbol{\beta_c}$) on the variance of short-run consumption shocks ($\sigma^2_{c,t-1}$) in equation (16).



Panel B: Posterior distribution of excess return loadings ($\boldsymbol{\beta_f}$) on the variance of shocks to the conditional consumption growth mean ($\sigma^2_{f.t-1}$) in equation (16).



Panel C: Posterior distributions of excess return loadings ($\boldsymbol{\beta_r}$) on the common financial return variance ($\sigma^2_{r.t-1}$) in equation (16).

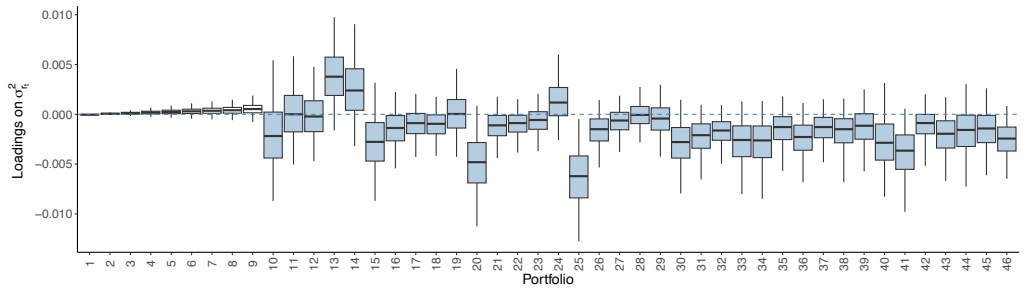


Figure 16. Loadings of excess returns on consumption and returns volatilities. This figure shows the box plots of the posterior distributions of the loadings of portfolio excess returns on the variance of short-run consumption shocks ($\sigma^2_{c,t-1}$), the variance of shocks to conditional consumption growth ($\sigma^2_{f,t-1}$), and the common financial returns variance($\sigma^2_{r,t-1}$). Portfolios are ordered with bonds first (1–9), Fama-French 25 size and book-to-market second (10–34), and industry portfolios last.

Table IV. Correlations among Stochastic Volatility Processes and VXO Index

The table summarizes the posterior mean and 2.5%, 5%, 50%, 95%, and 97.5% quantiles of the correlations among σ^2_{ct}, σ^2_{ft}, σ^2_{rt}, and the VXO index under a diffuse prior for the autoregressive coefficients of the vol processes.

	Mean	2.5%	5%	50%	95%	97.5%
Panel A: correlations of vol processes with VXO^2 index						
$cor(\sigma^2_{ct}, VXO^2_t)$	0.16	-0.05	-0.02	0.16	0.37	0.41
$cor(\sigma^2_{ft}, VXO^2_t)$	0.44	0.22	0.26	0.45	0.61	0.64
$cor(\sigma^2_{rt}, VXO^2_t)$	0.21	0.09	0.11	0.19	0.36	0.39
Panel B: Pairwise correlations of vol processes						
$cor(\sigma^2_{ct}, \sigma^2_{ft})$	0.08	-0.09	-0.07	0.07	0.27	0.32
$cor(\sigma^2_{ct}, \sigma^2_{rt})$	0.09	-0.04	-0.03	0.07	0.28	0.34
$cor(\sigma^2_{ft}, \sigma^2_{rt})$	0.10	-0.03	-0.02	0.07	0.32	0.41

Table VI, Panel A. What Drives the Consumption Shocks Spanned by Financial Markets?

This table presents correlation coefficients between f_t and the Fama-French five factors as well as the first five PCs of asset returns. We report 95% posterior credible intervals under the coefficient estimates. In Panel A, the cross-section of base assets used to estimate f_t includes 25 size-and-value-sorted portfolios, 12 industry portfolios, and nine bond portfolios.

Panel A: Baseline stock and bonds cross-section					
	MKT	SMB	HML	RMW	CMA
Correlation	0.878	0.584	0.012	-0.195	-0.180
95% CI	[0.805, 0.935]	[0.476, 0.694]	[-0.144, 0.137]	[-0.242, -0.152]	[-0.304, -0.074]
	PC1	PC2	PC3	PC4	PC5
Correlation	0.936	0.184	-0.103	0.079	-0.010
95% CI	[0.874, 0.971]	[0.050, 0.291]	[-0.265, 0.068]	[-0.014, 0.180]	[-0.031, 0.012]

Table VII, Panels A–D. Implications for Structural Models

This table presents estimates of RRA, average implied annualized risk-free rate, and its annualized volatility using two cross-sections of asset returns: (i) 37 stock and nine bond portfolios and (ii) Kozak et al. (2020) 74 anomaly portfolios. The risk price of f_t (and its 90% confidence intervals), denoted by b_f, are from Table 5. Cumulative impulse responses of *nondurable* consumption growth, $\sum_{j=0}^{S} \rho_j$, are estimated using our MA model, with $\bar{S} = 14$ quarters. We consider specifications with and without SV. In models with SV, we assume three separate SV processes—$\sigma^2_{c,t}$, $\sigma^2_{f,t}$, and $\sigma^2_{r,t}$—all of which are allowed to drive conditional mean returns. In the CRRA case, the RRA coefficients are given by $\gamma_S = b_f / \sum_{j=0}^{S} \rho_j$, where $S \in \{0, 2, \ldots, 14\}$ (see equation (IA.44) in the Internet Appendix). In the Epstein-Zin case, we consider two different values of IES, $\psi \in \{0.5, 1.5\}$, and $\gamma = (b_f + \frac{1}{\psi} \sum_{j=1}^{\bar{S}} \kappa_z^j \rho_j)/(\rho_0 + \sum_{j=1}^{\bar{S}} \kappa_z^j \rho_j)$ (see equation (IA.54)). The mean and volatility of the risk-free rate are obtained using equations (IA.42) and (IA.48) of the Internet Appendix, where $\delta = 0.9965$ (following the quarterly calibration of Bansal et al. (2016, Table 6)). In Panels A to D, we consider aggregate nondurable consumption data.

	CRRA								Epstein-Zin	
	$S = 0$	2	4	6	8	10	12	14	$\psi = 1.5$	$\psi = 0.5$
Panel A. Aggregate consumption in 37 stock and nine bond portfolios (constant volatility)										
RRA	150.1	53.0	33.6	28.0	26.8	24.9	23.1	23.2	24.1	25.2
90% CI	[49.8, 244.3]	[17.6, 86.4]	[11.2, 54.8]	[9.3, 45.6]	[8.9, 43.6]	[8.3, 40.6]	[7.7, 37.5]	[7.7, 37.8]	[8.4, 38.8]	[9.5, 40.0]
$\mathbb{E}[r_f]$	24.24%	52.20%	39.03%	34.04%	32.91%	31.07%	29.22%	29.41%	1.77%	3.80%
$\sigma(r_f)$	109.51%	38.71%	24.54%	20.44%	19.56%	18.18%	16.82%	16.96%	0.49%	1.46%
Panel B. Aggregate consumption in 37 stock and nine bond portfolios (stochastic volatility)										
RRA	161.8	66.7	38.0	30.6	28.3	23.7	20.1	19.6	20.5	21.7
90% CI	[53.7, 263.4]	[22.1, 108.5]	[12.6, 61.8]	[10.2, 49.9]	[9.4, 46.1]	[7.9, 38.6]	[6.7, 32.7]	[6.5, 31.9]	[7.2, 33.0]	[8.4, 34.2]
$\mathbb{E}[r_f]$	35.03%	61.90%	43.89%	37.32%	35.11%	30.43%	26.53%	25.98%	1.79%	4.08%
$\sigma(r_f)$	164.87%	56.18%	30.00%	23.77%	21.88%	18.11%	15.21%	14.81%	0.50%	1.46%
Panel C. Aggregate consumption in Kozak et al. (2020) 74 anomaly portfolios (constant volatility)										
RRA	150.7	42.6	27.7	21.7	19.9	17.7	16.0	15.7	16.5	17.7
90% CI	[67.3, 235.4]	[19.0, 66.5]	[12.4, 43.2]	[9.7, 33.9]	[8.9, 31.1]	[7.9, 27.7]	[7.1, 24.9]	[7.0, 24.5]	[7.7, 25.5]	[8.9, 26.7]
$\mathbb{E}[r_f]$	44.65%	47.59%	34.42%	28.28%	26.30%	23.87%	21.83%	21.55%	1.80%	4.27%
$\sigma(r_f)$	126.13%	35.66%	23.14%	18.17%	16.65%	14.84%	13.35%	13.15%	0.56%	1.67%
Panel D. Aggregate consumption in Kozak et al. (2020) 74 anomaly portfolios (stochastic volatility)										
RRA	159.7	46.4	30.2	22.1	19.5	16.8	14.6	14.4	15.2	16.4
90% CI	[71.3, 249.4]	[20.7, 72.4]	[13.5, 47.2]	[9.9, 34.6]	[8.7, 30.5]	[7.5, 26.2]	[6.5, 22.8]	[6.4, 22.4]	[7.1, 23.4]	[8.3, 24.6]
$\mathbb{E}[r_f]$	41.64%	50.78%	37.09%	28.83%	25.96%	22.86%	20.29%	20.00%	1.67%	4.58%
$\sigma(r_f)$	158.52%	40.89%	26.18%	19.00%	16.71%	14.33%	12.43%	12.22%	0.61%	1.71%

REFERENCES

Bansal, Ravi, Dana Kiku, and Amir Yaron, 2016, Risks for the long run: Estimation with time aggregation, *Journal of Monetary Economics* 52–69.

Box, G. E. P., and David A. Pierce, 1970, Distribution of residual autocorrelations in autoregressive-integrated moving average time series models, *Journal of the American Statistical Association* 65, 1509–1526.

Bryzgalova, Svetlana, Jiantao Huang, and Christian Julliard, 2026, Consumption in asset returns, *Journal of Finance* 81, 2271–2330.

Fama, Eugene F., and Kenneth R. French, 1992, The cross-section of expected stock returns, *Journal of Finance* 47, 427–465.

Kozak, Serhiy, Stefan Nagel, and Shrihari Santosh, 2020, Shrinking the cross-section, *Journal of Financial Economics* 135, 271–292.

Ljung, G. M., and G. E. P. Box, 1978, On a measure of lack of fit in time series models, *Biometrika* 65, 297–303.

Newey, Whitney K., and Kenneth D. West, 1987, A simple, positive semidefinite, heteroskedasticity and autocorrelation consistent covariance matrix, *Econometrica* 55, 703–708.